

Metastable phases in vapour-deposited Al–Ru alloys

ZARIFF A. CHAUDHURY, C. SURYANARAYANA

Department of Metallurgical Engineering, Banaras Hindu University, Varanasi-221 005, India

Vapour deposition of two Al–Ru alloys containing 10 and 15 wt % Ru resulted in the formation of supersaturated solid solutions. Electron microscopy and electron diffraction techniques have been used to characterize this as-quenched structure and also those formed on subsequent decomposition. Elevated-temperature (~ 650 – 800 K) annealing treatments resulted in the formation of a metastable intermediate phase. Electron diffraction evidence suggested that this phase can be assigned a simple cubic structure either of the Mo_3N_2 -type with $a = 0.42$ nm or of the $\text{Mg}_2\text{Zn}_{11}$ -type with $a = 0.84$ nm. Further annealing led to the formation of the equilibrium Al and Al_6Ru phases. The morphology and structural features of transformation products and the crystal structure details of the metastable intermediate phase have been discussed.

1. Introduction

The rapid quenching of metallic melts has been found to result in refinement of grain size, formation of supersaturated solid solutions and production of metastable crystalline and amorphous phases ([1], eg. [2]). Vapour deposition has also been found effective in producing metastable effects [3]. However, only a few comparative investigations have been carried out on rapid quenching and vapour deposition [4–8] to try to understand the similarities and/or differences between the products. The limited results available so far indicate that the same metastable effects need not be observed in both the cases. The difference can be attributed, at least in part, to the mechanism of formation of such phases. During vapour deposition, the phases form directly from the vapour by an atom-by-atom deposition process and the metastable phases produced by this technique may not be easily realized by liquid quenching. We recently undertook an extensive and detailed investigation on the constitution of aluminium-rich aluminium–ruthenium alloys subjected to melt quenching [9]. It has been observed that the solid solubility of ruthenium in aluminium can be increased from the equilibrium value of less

than 0.1 wt %* to between 10 and 15% by melt quenching. Furthermore, a metastable Al_2Ru phase with a CaF_2 -type cubic structure was also found to form during decomposition of the supersaturated solid solutions. With a view to comparing the results of melt quenching and vapour deposition, we vapour deposited two Al-rich Al–Ru alloys and the results are described in this paper.

Several intermediate phases have been reported to form under equilibrium conditions in the Al–Ru system [10]. The most Al-rich intermediate phase is Al_6Ru followed by $\text{Al}_{13}\text{Ru}_4/\text{Al}_3\text{Ru}$, Al_2Ru , Al_3Ru_2 and AlRu . Thus, in the alloys used in the present investigation, the equilibrium constitution is a mixture of Al and Al_6Ru . Another intermediate phase with the composition Al_{12}Ru has been detected by Obrowski [11], but has not been confirmed by others (see also [9]).

2. Experimental procedure

Two Al–Ru alloys containing nominally 10 and 15% Ru were prepared as described earlier [9] and were vapour deposited on to “formvar”-coated copper grids at room temperature. The alloys were flash evaporated from a tantalum boat under a high vacuum of 10^{-6} Torr. Sufficient quantity of

*All compositions are expressed in weight percent in this paper unless otherwise stated.

the alloys was taken to produce thin films about 100 nm thick. The as-deposited films were examined in a Philips EM 300 transmission electron microscope operating at 100 kV and fitted with a goniometer stage.

The vapour-deposited films were given appropriate annealing treatments after encapsulating them in quartz capsules under high vacuum. Some specimens were also transformed *in situ* in the electron microscope using a hot-stage specimen holder. Both the types of film were characterized under diffraction and imaging modes.

3. Results and discussion

3.1. Supersaturated solid solutions

Fig. 1 shows a bright-field electron micrograph of the as-deposited structure of an Al–10% Ru alloy film and the corresponding diffraction pattern is shown as an inset. From the micrograph it is clear that all the ruthenium has dissolved in aluminium to form the solid solution. The electron diffraction pattern clearly reveals the presence of a single fcc phase. Formation of such a supersaturated solid solution is observed in the Al–15% Ru alloy as well.

The grain size of the supersaturated solid solution in the as-deposited condition is extremely small, measuring only about 30 nm. Such fine grain sizes are not unusual in vapour-deposited thin films. For example, Cantor and Cahn [4, 5] report a value as small as 5 nm for their films. Fig. 2 shows a micrograph depicting the fine grain size more clearly in an Al–15% Ru alloy. The grain size here also is only about 30 nm. The lattice parameter of the solid solution calculated

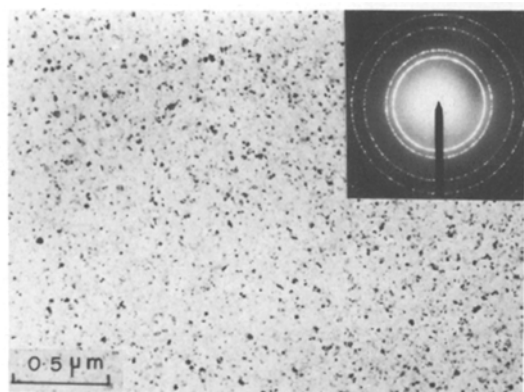


Figure 1 Microstructure of as-deposited Al–10% Ru alloy film showing the formation of a supersaturated solid solution of ruthenium in aluminium. The diffraction pattern is shown inset.

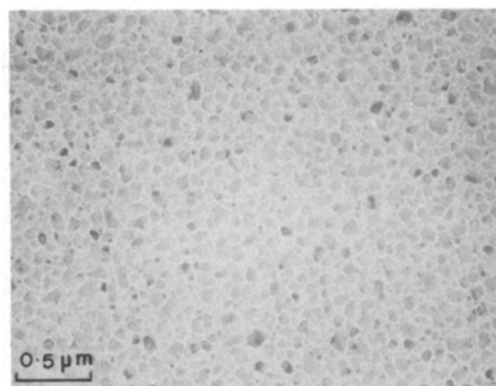


Figure 2 Electron micrograph of as-deposited Al–15% Ru alloy. Notice the clear grain formation.

from electron diffraction patterns works out to be 0.402 and 0.383 nm for the alloys containing 10 and 15% Ru, respectively. Although, a high accuracy cannot be achieved in calculations of lattice parameters from electron diffraction patterns, the decreasing values clearly indicate an increased ruthenium content in the solid solutions.

Some of the thin films were heated directly with the intense electron beam to detect any possible changes in structure. Fig. 3 shows a microstructure, wherein, apart from grain growth, there has not been any other observable change. The grain size at this stage is about 80 nm.

Some films have also been heat treated externally under a high vacuum at different temperatures. During these experiments, it was noticed that there was only grain growth up to 623 K. Fig. 4a shows the micrograph of a film annealed for 60 min at this temperature. Two points are worth noting in this micrograph. Firstly, the grain

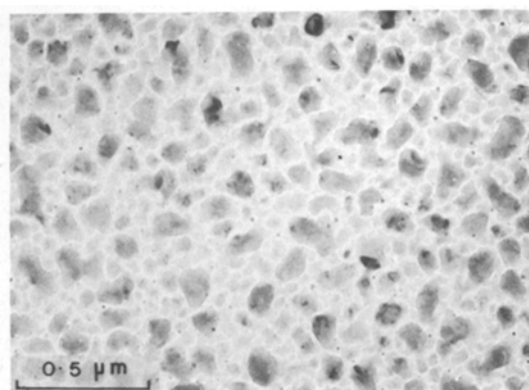


Figure 3 Grain growth observed during *in situ* heating of the supersaturated solid solution.

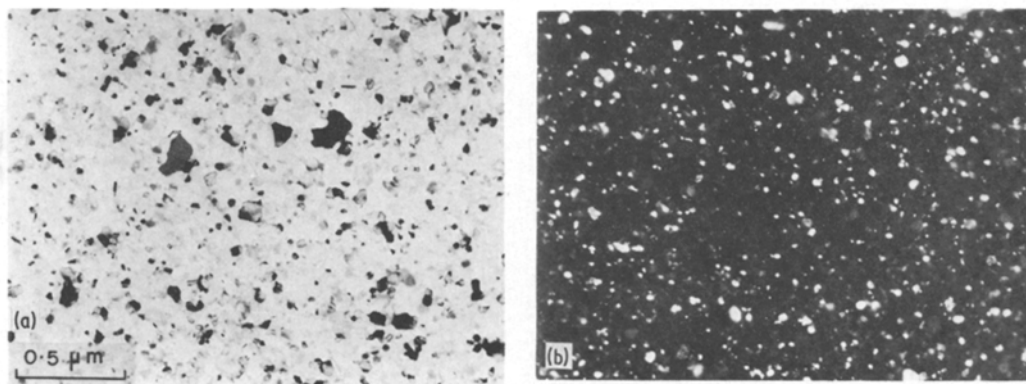


Figure 4 (a) Bright-field electron micrograph of the Al-10% Ru alloy film heat treated for 60 min at 623 K. (b) The corresponding dark-field picture.

boundaries are very sharp and clear and the grains measure about 100 nm in size. Secondly, this size is different from the 80 nm size detected during continuous heating using the electron beam. The dark-field electron micrograph in Fig. 4b brings out this fact clearly.

It is often claimed that vapour deposition results in a higher rate of cooling compared to melt quenching, and as such it is easy to produce an amorphous phase more easily. However, the stability of these amorphous phases is extremely low; normally they crystallize at temperatures well below room temperature. In the present investigation, the substrate has been kept at room temperature to provide comparable conditions between vapour deposition and melt quenching. Furthermore, the size difference between Al (0.286 nm) and Ru (0.265 nm) atoms, being only about 7%, is not conducive to the formation of an amorphous phase in the Al-Ru system.

It has been mentioned above that supersaturated

solid solutions have been obtained in both the alloys by vapour deposition. This result should be compared with that obtained by melt quenching [9, 12] wherein solid solubility extensions in Al have been achieved only up to about 11% Ru. Thus, vapour deposition appears to be a more powerful technique in achieving supersaturations. Similar results have also been reported in Al-Pd [8] and Al-Rh [13] systems.

3.2. Decomposition behaviour

It has been mentioned in the previous section that the supersaturated solid solution has been found to be stable up to 623 K. Annealing the thin films at higher temperatures resulted in the precipitation of intermetallic compounds. Typical results obtained during decomposition at 773 K are presented below.

Fig. 5 shows the morphologies of the precipitate formed. It can be either in the form of needles (Fig. 5a) or as massive particles (Fig. 5b). Electron

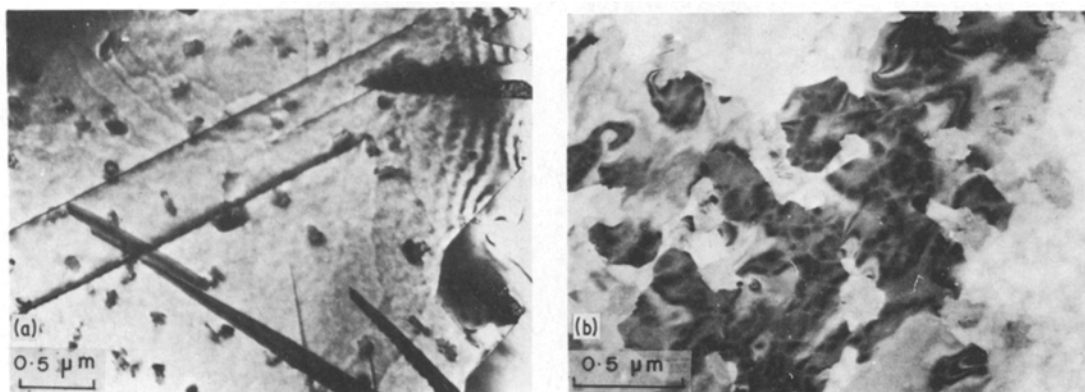


Figure 5 Precipitation of Al₆Ru phase from the supersaturated solid solution on annealing at 773 K for 60 min. (a) The needle-like shape, and (b) the massive shape.

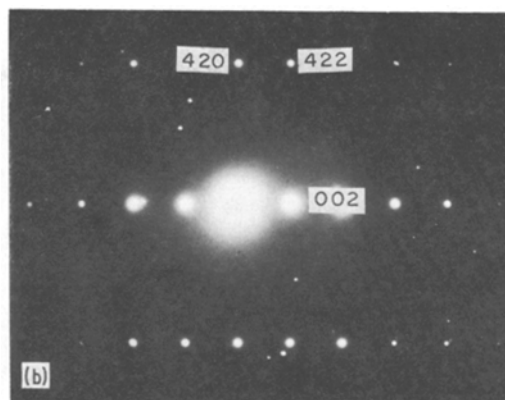
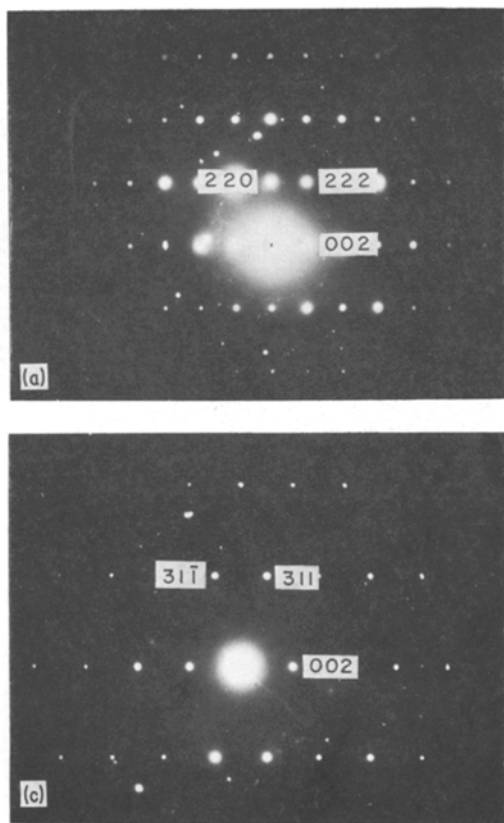


Figure 6 Electron diffraction patterns from the Al_6Ru phase. (a) $[1\bar{1}0]$, (b) $[1\bar{2}0]$ and (c) $[1\bar{3}0]$ zones.

diffraction patterns (Fig. 6) from these particles aided in unambiguously identifying the precipitate as the equilibrium Al_6Ru phase having an orthorhombic structure with $a = 0.7489$ nm, $b = 0.6556$ nm and $c = 0.8961$ nm. Yet another morphology of the Al_6Ru phase is shown in Fig. 7. Even though the microstructure resembles a spinodal transformation product, the diffraction pattern coupled with the dark-field micrograph (Fig. 7b) revealed that this is only the Al_6Ru phase. Investigations on several films suggested

that the massive shape is the more common morphology indicating that the interconnected “noodle”-like structure (Fig. 7) is perhaps the early transformation product.

Although the above sequence is observed in many areas of the films, it has been noticed that another intermediate phase precipitated out in other regions. Fig. 8a shows the characteristic lath morphology of the phase and Fig. 8b to d shows the typical diffraction patterns from this phase. These diffraction patterns cannot be indexed on the basis of any of the known intermediate phases in the Al–Ru system. By trial and error, it has been possible to index all the diffraction patterns from this phase as arising from a simple cubic lattice with $a = 0.42$ nm. However, it is worth noting that Fig. 8d shows that some type of ordering is taking place in this phase. Since such a structure is not found under equilibrium conditions, this can be considered a

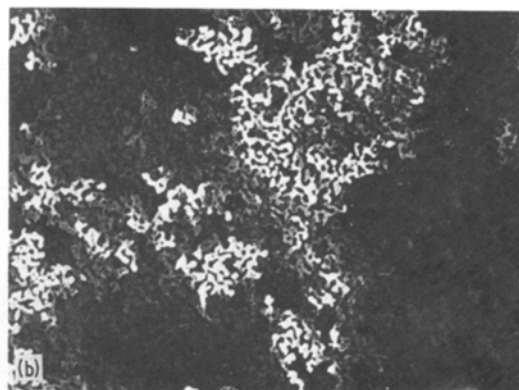
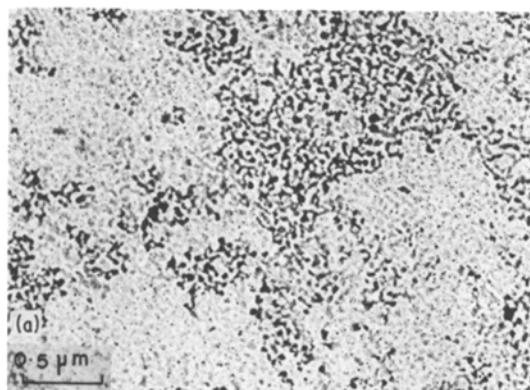


Figure 7 (a) Interconnected “noodle”-like morphology of the Al_6Ru phase. (b) The corresponding dark-field picture.

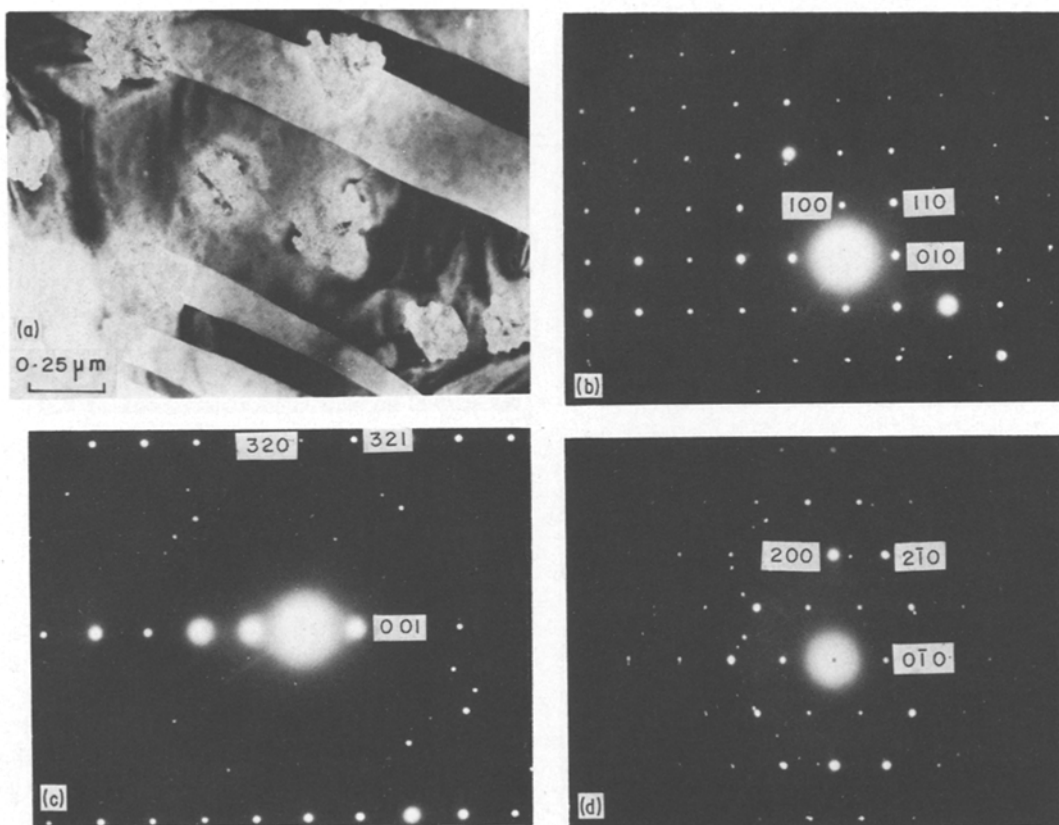


Figure 8 (a) Characteristic lath morphology of the metastable intermediate phase. (b)-(d) Typical electron diffraction patterns from this phase: (b) [001]; (c) [230]; (d) [001] zones.

metastable intermediate phase. Furthermore, this phase does not correspond to any of the nitrides, oxides or other compounds based on Al and/or Ru. Long annealing treatments have invariably led to the equilibrium constitution of Al + Al₆Ru in all the films investigated. To sum up, it can be mentioned that the supersaturated solid solution transforms to the equilibrium phases via the formation of a metastable phase.

3.3. Nature of the metastable intermediate phase

The formation of metastable phases during decomposition of supersaturated solid solutions is of common occurrence. Hence, it is not surprising that in the present system also a metastable intermediate phase formed prior to the formation of equilibrium phases. As already mentioned, this phase could be assigned a simple cubic structure with $a = 0.42$ nm. On the basis of this, the unit cell volume works out as 0.074 nm³. Fig. 9 shows a plot of the mean atomic volume of the equilibrium intermediate phases in the Al–Ru system as a

function of Ru content. The mean atomic volumes of pure Al and pure Ru are joined by a dashed line. From the generally observed negative deviation of the atomic volume, it is reasonable to assume that the unit cell of the present metastable phase contains five atoms having a mean atomic volume of 0.0148 nm³. Thus, this phase can be assigned a composition corresponding to Al₄Ru or Al₃Ru₂. The available literature on crystal structures [10] shows that some of the A₄B-type phases and some A₃B₂-type phases have cubic structures. From the mean atomic volume plot shown in Fig. 9, it is clear that the atomic volume of 0.0148 nm³ corresponding to a composition of 40 at. % Ru gives an excellent fit and suggests that this phase may have the formula Al₃Ru₂. γ -Mo₃N₂ in thin film form has a simple cubic structure [14] and thus, the present metastable Al₃Ru₂ phase can be considered a prototype of γ -Mo₃N₂.

As pointed out earlier, some type of ordering is detected in Fig. 8d. However, if one doubles the lattice parameter to $a = 0.84$ nm, the extra reflections can also be satisfactorily explained.

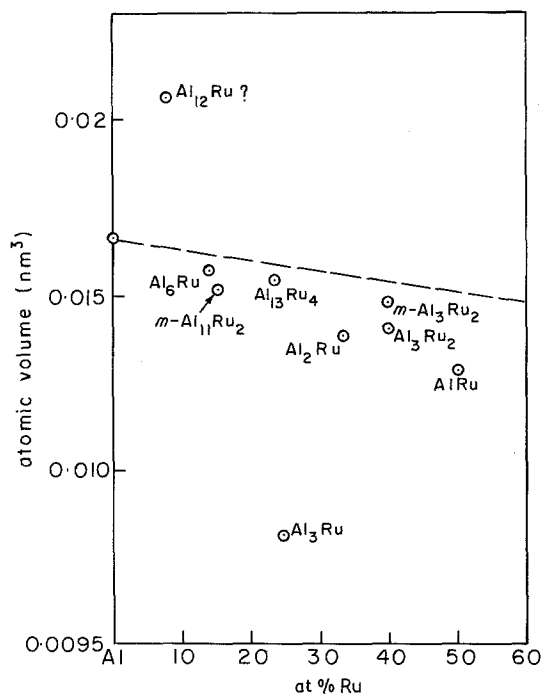


Figure 9 Plot of mean atomic volume of the intermediate phases in the Al–Ru system.

In this case, it is possible that this phase is isotypic with the $\text{Mg}_2\text{Zn}_{11}$ -type cubic structure containing 39 atoms per unit cell [15]. On this basis, the atomic volume works out as 0.0152 nm^3 and this also fits exceedingly well the variation of mean atomic volume with Ru content (Fig. 9). In this case, the chemical formula for the metastable phase will be $\text{Al}_{11}\text{Ru}_2$.

Since both the cubic structures satisfactorily explain the diffraction patterns, it is rather difficult to choose between the two. In this connection the following points are worth considering.

$\gamma\text{-Mo}_3\text{N}_2$ structure was observed only in thin films and characterized by electron diffraction. Such a phase is not detected in bulk alloys. Furthermore, the ratio of the sizes of Mo to N atoms is almost double that of Al to Ru, which casts a shadow of doubt on the suitability of Mo_3N_2 as a prototype for the present metastable phase. In favour of the Mo_3N_2 -type structure it should be mentioned that under equilibrium conditions Al_3Ru_2 has a trigonal Al_3Ni_2 -type structure which is quite complex compared with the cubic structure proposed in the present investigation. Anseau [6] has clearly pointed out that simple structures are preferentially formed during vapour deposition.

On the other hand, if one assumes that the present phase has the $\text{Mg}_2\text{Zn}_{11}$ -type cubic structure, the reflections indexed as $\{100\}$ will be $\{200\}$ type and there is no reason why $\{100\}$ reflections should have been absent in Fig. 8b and c. All the reflections present in Fig. 8d will be, however, explained without invoking the presence of superlattice reflections. The size ratio of Mg to Zn is comparable to that of Al to Ru. The only problem, in fact, will be the absence of reflections of the $\{100\}$ type in Fig. 8b and c and, in addition, (200) in Fig. 8d. It may be pertinent here to recall that the intensity of the $\{100\}$ reflections in the $\text{Mg}_2\text{Zn}_{11}$ -type structure is relatively weak.

It has not been possible to record X-ray diffraction patterns from these thin films and thus the present indexing is tentative. Both types of structures seem to be equally appropriate. Both are cubic structures and thus this result is also consistent with the observation made by Anseau [6].

4. Conclusions

On the basis of our present investigation, the following conclusions can be drawn.

(1) The solid solubility of ruthenium in aluminium can be increased by vapour deposition at least up to 15%, while a solubility limit of only about 11% is achieved by melt-quenching.

(2) The metastable solid solution is stable up to 623 K beyond which temperature, precipitation takes place.

(3) Formation of equilibrium phases is preceded by the occurrence of a metastable phase. Electron diffraction evidence aided in identifying the structure of this phase as cubic of either the $\gamma\text{-Mo}_3\text{N}_2$ -type with $a = 0.42\text{ nm}$ or of the $\text{Mg}_2\text{Zn}_{11}$ -type with $a = 0.84\text{ nm}$. This is in contrast to the formation of a cubic Al_2Ru phase during the decomposition of supersaturated solid solutions obtained by melt-quenching.

(d) The equilibrium constitution in all the alloys is a mixture of Al and orthorhombic Al_6Ru phases.

Acknowledgements

The authors would like to thank the Head, Department of Metallurgical Engineering, Banaras Hindu University, for provision of laboratory facilities and Professor T.R. Anantharaman for encouragement. One of the authors (Z.A.C.)

wishes to thank the Ministry of Education and Culture, Government of India, for the award of a fellowship under the Indo-Bangladesh Cultural Exchange Programme.

References

1. C. SURYANARAYANA, "Rapidly Quenched Metals - A Bibliography 1973-1979" (IFI Plenum, New York, 1980).
2. Proceedings of the Fourth International Conference on Rapidly Quenched Metals, edited by T. Masumoto and K. Suzuki (Japan Institute of Metals, Sendai, 1982).
3. K. L. CHOPRA, "Thin Film Phenomena" (McGraw-Hill, New York, 1969).
4. B. CANTOR and R. W. CAHN, *Acta Metal.* **24** (1976) 845.
5. *Idem*, *J. Mater. Sci.* **11** (1976) 1076.
6. M. R. ANSEAU, *ibid.* **9** (1974) 1189.
7. M. G. SCOTT and R. MADDIN, "Rapidly Quenched Metals", edited by N. J. Grant and B. C. Giessen (M.I.T. Press, Cambridge, USA, 1976) p. 249.
8. G. V. S. SASTRY, C. SURYANARAYANA and G. VAN TENDELOO, *Phys. Stat. Sol.* **72** (1982).
9. Z. A. CHAUDHURY, G. V. S. SASTRY and C. SURYANARAYANA, *Z. Metallkde.* **73** (1982) 201.
10. W. B. PEARSON, "A Handbook of Lattice Spacings and Structures of Metals and Alloys", Vol. 2 (Pergamon Press, Oxford, 1967).
11. W. OBROWSKI, *Metall.* **17** (1963) 108.
12. A. N. VARICH and R. B. LYUKEVICH, *Izv. Akad. Nauk SSSR Metall* **1** (1973) 112.
13. Z. A. CHAUDHURY and C. SURYANARAYANA, *Thin Solid Films* in press.
14. N. V. TROICKAJA and Z. G. PINSKER, *Sov. Phys. Crystallogr.* **4** (1959) 33.
15. S. SAMSON, *Acta Chem. Scand.* **3** (1949) 835.

*Received 22 January
and accepted 22 March 1982*